NASA Technical Memorandum 88972

Four Spot Laser Anemometer and Optical Access Techniques for Turbine Applications

Mark P. Wernet
Lewis Research Center
Cleveland, Ohio

Prepared for the
12th International Congress on Instrumentation in Aerospace Simulation Facilities
cosponsored by the IEEE Aerospace and Electric Systems Society and NASA Langley Research Center
Williamsburg, Virginia, June 22-25, 1987

NASA

FOUR SPOT LASER ANEMOMETER AND OPTICAL ACCESS TECHNIQUES FOR TURBINE APPLICATIONS

Mark P. Wernet

National Aeronautics and Space Administration
Lewis Research Center
Cleveland, Ohio 44135

Abstract

A new time-of-flight anemometer (TOFA) system, utilizing a spatial lead-lag filter for bipolar pulse generation has been constructed and tested. This system, called a Four Spot Laser Anemometer, was specifically designed for use in high speed, turbulent flows in the presence of walls or surfaces. The new TOFA system uses elliptical spots to increase the flow acceptance angle to be comparable with that of a fringe type anemometer. The tightly focused spots used in the Four Spot yield excellent flare light rejection capabilities. Good results have been obtained to 75 μm normal to a surface, with an f/2.5 collecting lens. This system is being evaluated for use in a warm turbine facility. Results from both a particle lag velocity experiment and boundary layer profiles will be discussed. In addition, an analysis of the use of curved windows in a turbine casing will be presented. Curved windows, matching the inner radius of the turbine casing, preserve the flow conditions, but introduce astigmatic aberrations. A correction optic has been designed that virtually eliminates these astigmatic aberrations throughout the intrablade survey region for normal incidence.

Introduction

A laser anemometer offers a nonintrusive method for obtaining flow field information. Particles entrained in the flow provide scattering centers for the incident light. There are two common techniques for optically coding the measurement region. The Laser Fringe Anemometer (LFA) employs a sinusoidally varying fringe pattern. Knowledge of the fringe spacing and the detected signal frequency of particles traversing the measurement region permits the determination of the velocity component normal to the fringes. Another technique for encoding the measurement region (Time-Of-Flight Anemometer, TOFA) uses two closely spaced spots, where the flow velocity component parallel to the axis of the spots is obtained from the time-of-flight of particles traversing the two spots.

The motivation for this work was the desire for an anemometer capable of measurements near walls in turbulent flows. This requires a laser anemometer with special qualities. The optimum anemometer would have a wide acceptance angle to enable measurements of wide flow angle variations, and also have a high on-axis spatial selectivity, to limit unwanted flare light scattered from surfaces from reaching the detector. The LFA typically has a wider acceptance angle than a conventional TOFA system. This reduces the utility of TOFA systems in turbulent flows. However, the TOFA receiver can have much better on-axis spatial resolution than the LFA for the same f/number system.

In this work we describe testing of a new, modified TOFA system that has been constructed and tested for turbulent flow measurements in the presence of walls. The new TOFA system uses elliptical spots to increase the flow acceptance angle to be comparable to that of an LFA. Also, the new TOFA uses an optical code that vastly simplifies the pulse detection processor. A simple electronic pulse position technique was used instead of the more complex correlation techniques.[1-3] Results from both a particle lag velocity experiment and boundary layer profiles taken using the Four Spot TOFA will be discussed.

In addition to the laser anemometer data to be discussed, an analysis of the use of curved windows in a turbine casing will be presented. Curved windows, matching the inner radius of the turbine casing, preserve the flow conditions, but introduce astigmatic aberrations. A zoom correction optic has been designed that virtually eliminates these astigmatic aberrations throughout the intrablade survey region for normal incidence.

Four Spot Laser Anemometer

The electronic signal obtained from a normal two-spot TOFA system consists of two noisy gaussian shaped pulses separated by the transit time of a particle traversing the two light spots in the measurement region. An estimate of the peak to peak time of flight and knowledge of the spot spacing then yields the particle velocity component along the axis of the two spots. The inherent

noise on any type of photon detection system decreases the abilitv of the signal processor to determine the exact time-of-occurrence of a pulse. The particle's time-of-flight can be obtained more accurately by transforming the unipolar pulse into a bipolar pulse. The zero crossings of the bipolar pulses yield the estimated time-of-flight. The transformation from a unipolar to a bipolar pulse should not introduce additional noise to the signal. Lading[4] analyzed the performance of four methods for generating bipolar pulses: the derivative operator, Hilbert transforms, and both the spatial and temporal lead-lag filter. The results of his analysis showed that an advantage could be obtained by implementing the lead-lag filter spatially, before photon detection. The advantage of the spatial lead-lag filter is that the dimensions are fixed in space, but the temporal scale of the signal depends on the velocity. Thus, a spatial implementation will behave as an adaptive temporal lead-lag operator. The transformation to a bipolar pulse is thus made without adding noise to the signal and in a robust manner that does not depend on electronic delays. The Four Spot Anemometer system described herein has a spatial lead-lag filter.[5]

Implementation

The Four Spot TOFA system uses two pairs of partially overlapping spots in the measurement region. These two pairs of spots, labeled A to D, are separated by a distance X_0, orthogonally polarized, and partially overlapping (Fig. 1). The amount of overlap is, 2σ, where σ is the standard deviation of the e^{-2} gaussian spot width. The use of elliptical spots increases the acceptance angle of the measurement region-comparable to that of a laser fringe anemometer.

The transmitting section of the system contains two quarter-wave plate/Wollaston prism pairs (Fig. 2). The input light is linearly polarized. A cylindrical lens L_1 transforms the circular input beam into an elliptical beam. The first quarter-wave plate/Wollaston prism pair Q_1/W_1. Generates two angularly diverging, orthogonally polarized beams. These plane polarized beams are imaged by L_2 and L_3 onto the second pair Q_2/W_2. The first pair Q_1/W_1 must be at the back focal plane of L_2, and Q_2/W_2 must be at the front focal plane of L_3 to maintain the sharpness of the imaged spots. Emerging from the Q_2/W_2 pair are four consecutively, orthogonally polarized beams. The angular divergence of these beams is transformed into a spatial separation by the lens L_4. The angular divergence imparted by the Q_1/W_1 pair creates the spatial separation X_0. The angular divergence imparted by Q_2/W_2 creates the partially overlapping spots in the measurement region.

The measurement region geometry is controlled by the input beam diameter, the angular divergences of W_1 and W_2, and by the focal length of L_4. The quarter-wave plates allow the equalization of the intensities of the four spots.

The backscatter system configuration collects the scattered light from the measurement region back along the axis of the transmitted beam. The use of two elevation mirrors M_1 and M_2 allows this coaxial configuration. The received image is magnified by the image pair L_4 and L_7. The rectangular mirror M_2 acts as a vertical spatial filter mask in the receiver. The received light is recombined into two pairs of totally overlapping spots by a third Wollaston prism, W_3, which has the same angular split as W_2. These two spots are then imaged onto the receiver mask consisting of two precision air slits. The two totally overlapping pairs of spots are separated by a polarization selective beam-splitting cube. Two right angle mirrored prisms are used to separate the spot pairs into four individual signals. The separated signals are detected by four RCA 8645 photomultiplier tubes.

The Four Spot TOFA has been constructed using optical erector components (Fig. 3). A mirror-type image rotator has been incorporated into the Four Spot TOFA. The image rotator is common to both the transmitter and receiver, and permits two-dimensional velocity scans by taking measurements at several angular orientations of the measurement volume. The Four Spot TOFA uses an Argon ion laser operating at 514.5 nm.

The probe volume dimensions of the Four Spot TOFA are:

Elliptical spot width, μm	10
Elliptical spot height, μm	97
Spot overlap, μm	5
Spot pair spacing, μm	108
Acceptance angle,	±43°

The probe volume dimensions were measured using a pinhole/photomultiplier tube assembly. The TOFA probe volume was scanned over the pinhole and the recorded photomultiplier tube dc current as a function of position was fit to a gaussian using the technique of nonlinear least squares. The e^{-2} widths and heights of the fitted gaussians were taken as the probe volume dimensions. The spot pair separation was determined from the difference in the peak locations of the measured spots.

Operation

The temporal separation of the bipolar pulses is determined by a high speed Emitter-Coupled Logic (ECL) zero crossing detection circuit. Figure 4 shows the signal processing electronics. There are six input signals to the pulse detection circuit: the A, D, A + B, A - B, C + D, and C - D signals. The circuit uses the A and D signals to determine the direction of the detected particle. The A + B and C + D signals are used to enable comparators to search for the zero crossings of the A - B and C - D signals, respectively. The amplitude where either the A + B or the C + D signal enables the comparator is the threshold level. A particle traversing

from the left, through the AB and then CD spot pairs yields an A + B signal, which enables the A + B comparator. The circuit finds the A - B zero crossing and then disables the A + B comparator until either the particle is detected at C + D or the time window expires. The time window is set as the maximum time the processor will wait for an event at the CD spot pair, that is, the slowest expected velocity, before resetting the circuit. The analogous process occurs for a particle traversing from the opposite direction, first enabling C + D. The circuit now searches for the C - D zero crossing and then disables the C + D comparator until either a particle is detected at A + B or, again, until the time window expires. This technique yields the flow direction and minimizes the number of false counts due to simultaneous particles in the measurement region and/or particles traversing only one of the spot pairs.

The ECL processor outputs start and stop pulses which are fed into a time analyzer. The start and stop pulses correspond to a particle traversing the two pairs of spots in the measurement region, that is, the time-of-flight. The time analyzer generates a voltage pulse (0 to 10 V) that is proportional in amplitude to the time difference between the start-stop pulses. These voltage pulses are then sent to an analog to digital converter (ADC). The digital words from the ADC are fed into the back plane of a TSI model 1998 master interface. The TSI module generates a time-between-data (TBD) word from the Four Spot data. Both the measured velocity and TBD are sent via a Direct Memory Access (DMA) interface to a PDP 11/44 computer for analysis. At each measurement position, 1000 velocity events and 1000 TBDs are recorded.

Particle Lag Velocity Experiment

The Four Spot Laser Anemometer sample volume contains approximately half the illuminated area of a typical fringe type anemometer. The higher light flux in the probe volume enables the Four Spot to measure smaller particles than an LFA. Detection of smaller particles is desirable, since they follow the flow more accurately. A particle velocity lag experiment was conducted to determine the range of particle diameters detectable by the Four Spot system.

In the particle velocity lag experiment, the velocity of particles entrained in the flow are measured downstream of a sonic nozzle. The gas accelerates through the nozzle, reaching Mach 1 at the exit. Particles greater in diameter than approximately 0.3 μm will lag behind the gas velocity at the nozzle exit.[6] The amount of velocity lag is proportional to the particle diameter. The gas velocity can be calculated from the plenum temperature and the pressure drop across the nozzle. Since the laser anemometer can only measure the velocity of the particles entrained in the flow, the particle lag velocity is directly obtained. The measured particle velocity histograms are converted to particle diameter histograms. The mean diameter and standard deviation of the sampled particles are then determined from the particle diameter histograms.

The seed particles used in this experiment were diagnostic latex spheres of 0.5 and 0.8 μm mean diameter, with relative standard deviations of less than 1 percent. The specific gravity of the diagnostic spheres was 1.05. The diagnostic spheres were suspended in methanol. A commercial atomizer supplied the seed particles to the upstream plenum section of the nozzle. In order to verify the complete evaporation of the methanol at the measurement plane, pure methanol, with no seed added, was run through the atomizer. No velocity events were recorded, verifying the solvent evaporation. The results of the particle lag experiment are shown in Table I and the corresponding velocity histograms are shown in Figs. 5 and 6.

The spread in the histograms is caused by both error in the measurement and agglomeration of the seed particles. The estimates of the mean particle diameter are biased to higher values than the true particle diameters because of these effects. The results from the analysis show that the Four Spot can detect particles down to at least 0.5 μm in diameter using elliptical spots.

Boundary Layer Profiles

Discrimination against light not originating at the focii of the TOFA beams is a very important characteristic of a practical anemometer. Light from particles not at the focal plane may have a different velocity from those at the focal plane, i.e., a gradient may be present, and thus a spread of velocities will be measured. One wishes to minimize this spread. Shot noise from light scattered from walls is the limiting factor in how close to a wall one can get and obtain a measurement of the flow velocity.

A practical test of an anemometer's spatial selectivity is obtained by operating the system in a flow near a surface. A laminar boundary layer flow field would supply the necessary measurement environment. The boundary layer thickness $\delta(x)$ was defined as the distance from the surface where the velocity reached 99 percent of the freestream velocity. Two experimental setups were used. A rectangular nozzle, 6 by 12 mm, with an access window, provided an environment similar to that encountered in a windowed engine casing. Measurements were made in the boundary layer forming off the back wall of the nozzle. The back wall was painted black to reduce the amount of flare light. The second setup consisted of a low velocity circular nozzle. A flat plate was placed parallel to the flow at the nozzle exit, perpendicular to the incident light. The flat plate had a smooth polished surface. These two setups yielded a measure of how close to a wall measurements can be obtained.

The transit time probability distributions were converted to velocity probability distributions, VPDS, using the known spot spacing. The velocity distributions were measured at sequential

stations along a line perpendicular to the plane of the surface. An increase in the variance of the VPDs measured inside the boundary layer above the freestream VPD variance, gives an estimate of the range of velocities present across the length of the sample volume. The mean velocities at each measurement position were fit to a cubic polynomial describing the boundary layer velocity profile. The variances of the VPDs were plotted versus distance from the surface.

The results of these boundary layer profiles are shown in Figs. 7 to 10. Figure 7 shows the mean velocity versus distance from the surface for the windowed nozzle flow. Measurements were obtained to 100 μm from the surface for this setup. Figure 8 shows the velocity variance versus position for the profile in Fig. 7. The threshold level in the signal processor was adjusted at each measurement position to minimize the background noise. This accounts for the variation in the measured velocity variances in this figure.

Figures 9 and 10 show the mean velocity and velocity variance versus position for the flat plate configuration respectively. The profile was made at 1 cm from the leading edge of the plate. Measurements were obtained to 75 μm from the surface of the plate. The threshold level was held constant for the entire profile. Figure 10 shows the expected behavior of increasing velocity variance inside the boundary layer as the magnitude of the velocity gradient increases.

The free stream velocity was kept relatively low to provide sufficiently thick laminar boundary layers. The contraction nozzles used to supply the flow fields were driven by the building service air. The low velocity limit restricts the pressure drop across the nozzle to approximately 0.1 psia. Fluctuations in the service air caused perturbations in the flow field. Some of the structures observed in these boundary layer profiles may be artifacts of the service air fluctuations.

Additional tests using the Four Spot TOFA in hot flows have been conducted.[7] The new system was compared to an LFA and a low acceptance angle TOFA system. These comparison measurements were made in a burner rig. The temperature, velocity and turbulence intensity in the burner rig were: 700 °C, 350 m/sec, and 8 percent respectively. A core turbine blade was mounted in the hot cross flow to provide a surface for surface proximity measurements, and to compare each system's flow angle resolving capabilities in high turbulence flows.

Optical Compensation for Curved Turbine Windows

In the application of laser anemometer systems, the flow fields under study are typically inside a container or within some bounding surfaces. Laser anemometer systems require line-of-sight optical access to the measurement region. In order to obtain optical access to the flow, these surfaces or boundaries must be either removed or replaced with windows. The thickness of the windows is set by the physical stresses present in the system of interest. The incident beam angle, window thickness, and the refractive index change across the interface will determine the refracted beam direction in accordance with Snell's law. Thin windows are the most desirable, i.e., these introduce the smallest amount of aberrations. For the simple case of thin planar windows at normal incidence, the aberrations are negligible. For the case of curved windows, the astigmatic aberrations caused by the window are no longer negligible.

In our particular application, we are concerned with obtaining intrablade passage two-dimensional velocity surveys in a warm turbine rig for validation of new computational fluid dynamics code. A portion of the turbine rig casing has been cut away and replaced with a curved window. The inner radius of the window is matched with that of the turbine casing. A curved window is used to minimize the disturbance to the flow. An alternative approach is to use planar windows. This minimizes the astigmatic aberrations, but does not insure preservation of the flow field.[8]

The turbine rig has a blade tip radius of 254 mm. There are two casing windows, 6.35 and 9.525 mm thick fused quartz. The two windows are used to obtain optical access to the rotor and stator stages respectively. The laser anemometer is mounted on a 3-axis computer controlled positioning table. An image rotator enables the rotation of the laser anemometer probe volume. The 3-axis table allows the laser anemometer probe volume to be scanned inside the turbine rig. The scanning range is from the inside surface of the window to the turbine hub, a range of 38.1 mm. The single component laser anemometer probe volume must be rotated and scanned over the specified range to obtain the desired two-dimensional velocity survey. A schematic diagram of the laser anemometer system and turbine rig assembly is shown in Fig. 11.

The curved turbine casing window acts as an astigmatic optic. The aberrations caused by this curved window would produce a focus shift of a laser anemometer probe volume as the beams were rotated through a range of angles. Some beam uncrossing would also occur for beam orientations between the vertical and horizontal axes of the window. The focus shift would cause a change in fringe spacing for a LFA, or a spot spacing variation in a TOFA. The beam uncrossing error would prevent the beams from overlapping in the LFA, or alter the angular orientation of a TOFA. These errors could partially be accounted for in the data analysis procedure, but gross physical changes in the probe volume size would affect the sampling statistics. In the following analysis, we show that through the use of a single, zooming correction optic, the aberrations induced by the turbine casing window can be minimized, even as the system scans through the blade passage.

In a laser anemometer system, the collection optics essentially determine the system performance. The transmitted beams in the laser

anemometer system are usually very near the optical axis. This allows the use of large f/number optics in the transmitter. A laser anemometer probe volume is usually on the order of 100 μm in diameter. The number of fringes and their spacing depends on the specific application. The sample volume characteristics require high quality optical components for near diffraction limited performance.

The laser anemometer receiver collects light over the full aperture of the collection optics. The use of low f/number optics in the receiver increases the light gathering power of the system. The laser anemometer system under study employs an Argon ion laser operating at 514.5 nm. A pair of lenses is common to both the transmitter and receiver. These optics, consisting of an f/5 and f/2.5, 100 mm diameter lens pair, were custom designed for diffraction limited performance at the 514.5 nm wavelength. Both lenses are three element air spaced, single glass types, BK7 and SSK1 respectively. The lenses are configured to yield an effective magnification of one half, with the f/2.5 lens facing the probe volume.

The correction optic was designed using a commercial lens design (CLD) package on an IBM PC AT.[9] The CLD allows the user to specify an optical system and select the variables to be used in the optimization. The optimization process requires that the user define a merit function for targeting the expected aberrations in the system. A preknowledge of these aberrations and their tolerable magnitudes was required for properly designing the merit function. The object and image scales used in the merit function were chosen to correspond to the actual dimensions in the laser anemometer system. For this particular case, merit function targets were used to minimize the astigmatism, maintain constant image magnification as the input object rotates through a circle, and to minimize the zonal spherical aberrations.

The merit function targeted these quantities at four positions of the laser anemometer probe volume inside the turbine rig. This zooming feature allowed the optimization of the corrector element over the full scanning range of the laser anemometer system. Targets were also used to restrict the traversing range of the correction optic (less than 60 mm due to space limitations), and to maintain a constant system f/number throughout the scanning range; all satisfied at full aperture of the collection optics.

The optimization procedure yielded a single element cylindrical correction optic, for use with the 9.525 mm window. A similar, weaker optical compensator was designed for use with the 6.35 mm casing window. The optimized position of the correction optic was behind the 500 mm focal length f/5 lens. Ideally, the correction optic would be placed far from the object plane to avoid additional aberrations introduced by glass imperfections. The CLD optimization procedure placed the correction optic in a range of 114 to 170 mm from the f/5 lens. This is sufficiently far from the object plane, and also satisfied the traversing range constraints imposed by the turbine rig assembly.

As the laser anemometer probe volume is mechanically scanned by the 3-axis positioning table through the blade passage, the correction optic will be translated by its own actuator. The correction optic position depends on the probe volume immersion depth through the casing window (Figs. 11 and 12). Note the difference in the relative position of the probe volume and the correction optic for these two figures. As the probe volume immersion is increased, the actuator independently adjusts the corrector position. The zoom optimization features of the CLD package permitted this active compensation scheme.

The correction optic minimized the astigmatism and zonal spherical aberration in the system. Of the four zoom positions, the worst aberrations were observed in the deepest scan position, near the rotor hub. At this position, the collected cone of light rays encompasses the largest area of the turbine window. The power variation between the sagittal and tangential planes becomes the most pronounced in this configuration. The optimal compensation is achieved by traversing the correction optic in a similar manner, so that when the largest aperture of the turbine window is being used, the correction optic is closest to the f/5 lens. The correction optic clear aperture in this configuration is 70 mm. This provides a stronger correction capability as the aberrations increase due to the use of a larger area of the turbine window.

The largest errors in the compensated optical system are a variation in crossing angle of 3 percent from the sagittal to the tangential planes. This variation in angle can be compensated for in the data analysis procedures. The maximum focus shift is approximately 20 μm. These errors are tolerable, where before the system would not be considered feasible for obtaining measurements through the curved turbine window.

Conclusion

The Four Spot TOFA has been shown to perform as predicted. The system's high spatial selectivity and large acceptance angle will enable measurements in the hostile warm turbine environment. The Four Spot TOFA is capable of detecting particles down to 0.5 μm in diameter, using elliptical spots. It should be noted that in low turbulence flows, the cylindrical lens in the Four Spot transmitter could be removed, which would produce four circular spots in the measurement region. The use of four circular spots would increase the light flux through the illuminated area by an order of magnitude. The increased light flux would make the Four Spot system more sensitive to smaller particles. Again, this modification would only be performed in a low turbulence flow, where the expected flow angle variation was less than the acceptance angle of the anemometer.

The optical compensation scheme presented reduces the aberrations induced by the curved turbine casing window to an acceptable level. Without the compensation the laser anemometer system could not obtain the desired two-dimensional intrablade survey. This compensation technique will be instrumented on the warm turbine facility at NASA Lewis Research Center.

References

1. M.J. Fisher and F.R. Krause, "The Crossed-Beam Correlation Technique," J. Fluid Mech., vol. 28, pp. 705-717, 1967.
2. W. Matthes, W. Riebold, and E. de Cooman, "Measurement of the Velocity of Gas Bubbles in Water by a Correlation Method," Rev. Sci. Inst., vol. 41, pp. 843-845, 1970.
3. T.S. Durrani and C.A. Greated, "Spectral Analysis and Cross-Correlation Techniques for Photon Counting Measurements in Fluid Flows," Appl. Opt., vol. 14, pp. 778-786, 1975.
4. L. Lading, "Estimating Time and Time-Lag in Time-of-Flight Velocimetry," Appl. Opt., vol. 22, pp. 3637-3643, 1983.
5. M.P. Wernet, and R.V. Edwards, "Implementation of a New Type of Time-of-Flight Laser Anemometer," Appl. Opt., vol. 25, pp. 644-648, 1986.
6. B.R. Maxwell, and R.G. Seasholtz, "Velocity Lag of Solid Particles in Oscillating Gases and in Gases Passing Through Normal Shock Waves," NASA TN D-7490, 1974.
7. M.P. Wernet, and L.G. Oberle; "Laser Anemometry Techniques For Turbine Applications," to be Presented at the ASME Gas turbine Conference, May 1987.
8. R. Schodl, "Laser Dual Beam Method for Flow Measurements in Turbomachines," ASME Paper 74-GT-157, Mar. 1974.
9. Genesee Computer Center, Inc., GENII-PC Reference Manual, July 1985.

Table I

Seed particle mean diameter, μm	Measured particle mean diameter, μm	Standard deviation of mean diameter, μm
0.50	0.54	0.20
.80	.82	.14

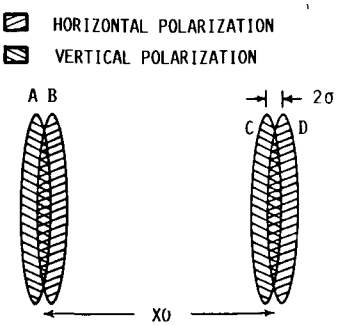

FIGURE 1. - FOUR SPOT TOFA MEASUREMENT VOLUME GEOMETRY. THE ORTHOGONALLY POLARIZED SPOTS OVERLAP BY 2σ. THE SPOT PAIRS ARE SEPARATED BY XO.

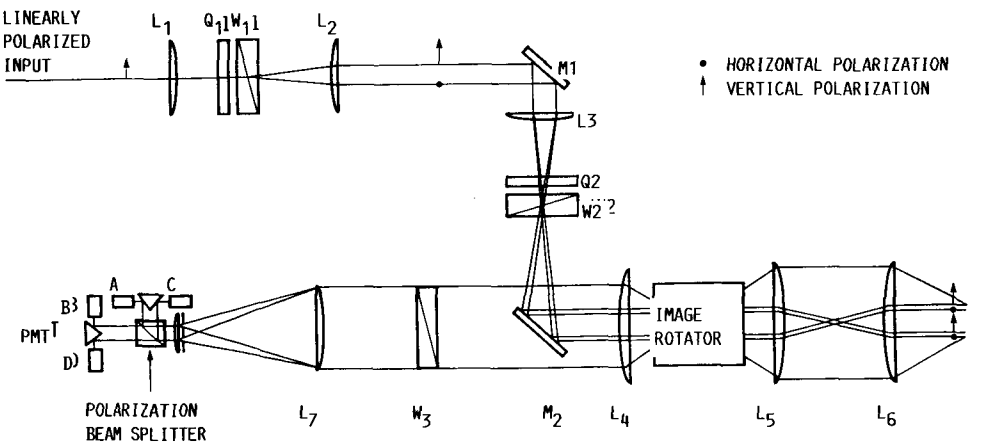

FIGURE 2. - SCHEMATIC VIEW OF THE TRANSMITTING AND RECEIVING OPTICS.

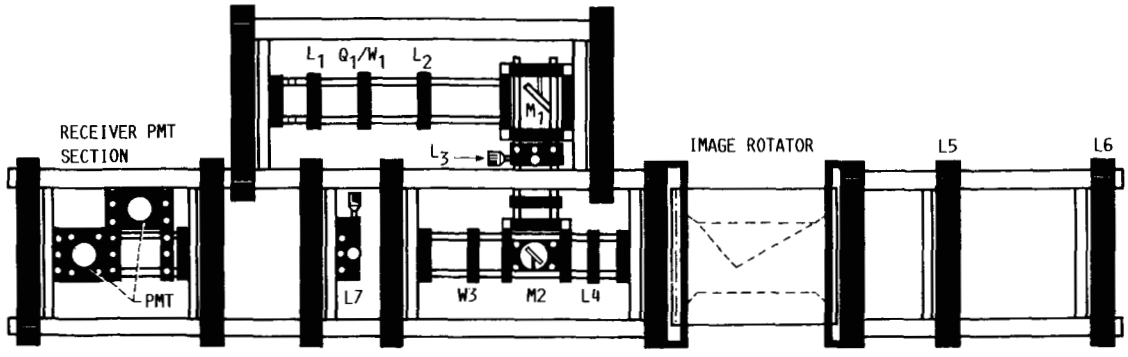

FIGURE 3. - FOUR SPOT ANEMOMETER SYSTEM CONSTRUCTED FROM OPTICAL ERECTOR COMPONENTS.

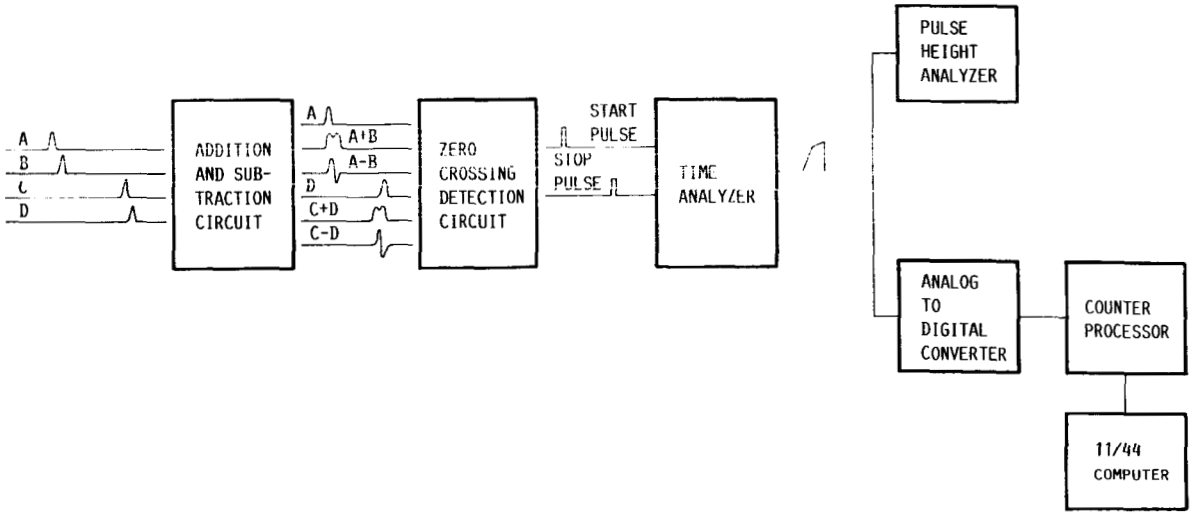

FIGURE 4. - SCHEMATIC DIAGRAM OF THE FOUR SPOT SIGNAL PROCESSING ELECTRONICS. THE FOUR INPUTS FROM THE PHOTOMULTIPLIER TUBES ARE USED TO GENERATE THE SIX INPUTS TO THE ZERO CROSSING DETECTION CIRCUIT. THE TIME ANALYZER GENERATES A VOLTAGE PULSE PROPORTIONAL TO THE PARTICLES TIME-OF-FLIGHT. THESE PULSES CAN BE DIGITIZED BY THE ADC AND SENT TO THE SYSTEM COMPUTER FOR STORAGE, OR SENT TO A PULSE HEIGHT ANALYZER FOR ON-LINE HISTOGRAM DISPLAY.

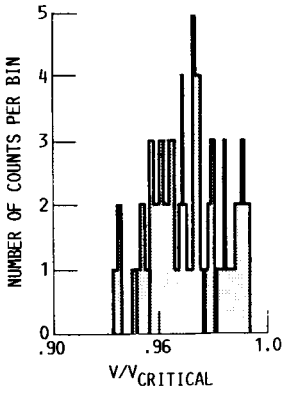

FIGURE 5. - PARTICLE LAG VELOCITY HISTOGRAM FOR 0.5 μM SEED PARTICLES. THE MEASUREMENT PLANE IS 200 μM FROM THE NOZZLE EXIT. THE VELOCITIES HAVE BEEN NORMALIZED BY THE CRITICAL VELOCITY, WHICH IS 315 M/SEC.

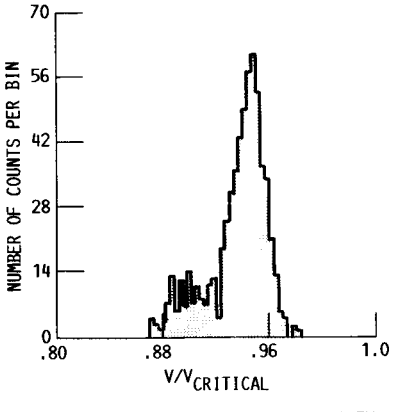

FIGURE 6. - PARTICLE LAG VELOCITY HISTOGRAM FOR 0.8 μM SEED PARTICLES. THE MEASUREMENT PLANE IS 200 μM FROM THE NOZZLE EXIT. THE VELOCITIES HAVE BEEN NORMALIZED BY THE CRITICAL VELOCITY, WHICH IS 315 M/SEC.

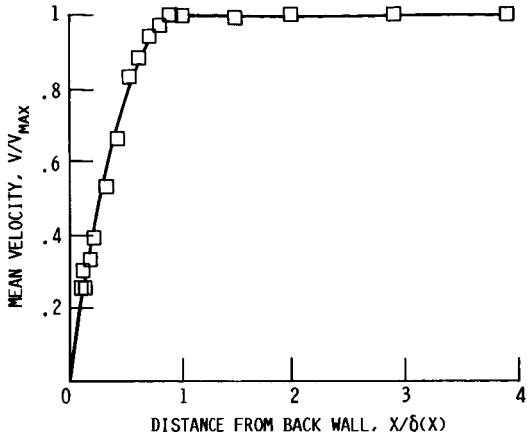

FIGURE 7. - WINDOWED NOZZLE BOUNDARY LAYER FLOW PROFILE. THE VELOCITIES ARE NORMALIZED BY THE FREE STREAM VELOCITY, WHICH IS 16.9 M/SEC. THE DISTANCE FROM THE SURFACE IS NORMALIZED BY THE ESTIMATED BOUNDARY LAYER THICKNESS, $\delta(x)$. THE MINIMUM APPROACH DISTANCE TO THE SURFACE IS 100 μM.

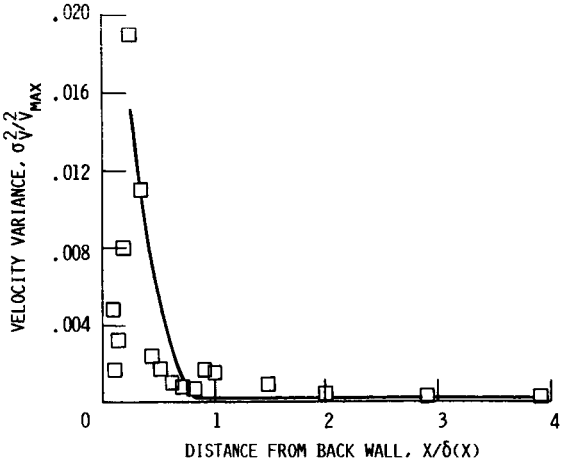

FIGURE 8. - VELOCITY VARIANCE FOR THE WINDOWED NOZZLE BOUNDARY LAYER FLOW. THE VARIANCE IS NORMALIZED BY THE FREE STREAM VELOCITY. THE DISTANCE FROM THE SURFACE IS NORMALIZED BY THE ESTIMATED BOUNDARY LAYER THICKNESS.

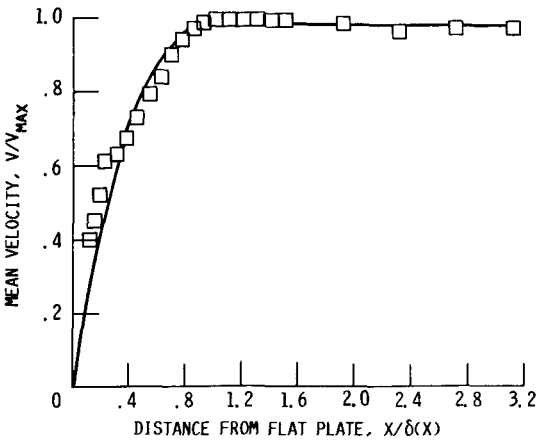

FIGURE 9. - FLAT PLATE BOUNDARY LAYER FLOW PROFILE. THE VELOCITIES ARE NORMALIZED BY THE FREE-STREAM VELOCITY, WHICH IS 12.4 M/SEC. THE DISTANCE FROM THE SURFACE IS NORMALIZED BY THE ESTIMATED BOUNDARY LAYER THICKNESS, $\delta(x)$. THE MINIMUM APPROACH DISTANCE TO THE SURFACE IS 75 μM.

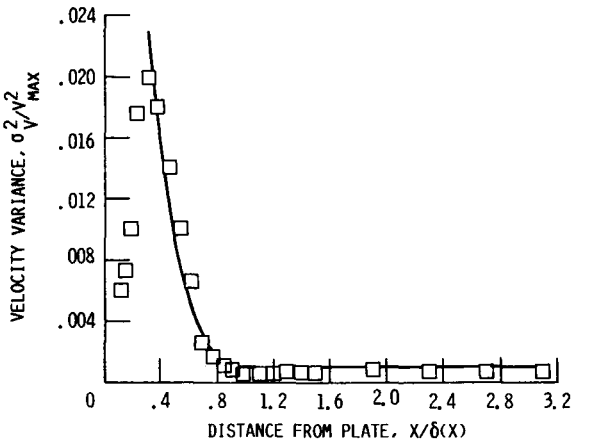

FIGURE 10. - VELOCITY VARIANCE FOR THE FLAT PLATE BOUNDARY LAYER FLOW. THE VARIANCE IS NORMALIZED BY THE FREE-STREAM VELOCITY. THE DISTANCE FROM THE SURFACE IS NORMALIZED BY THE ESTIMATED BOUNDARY LAYER THICKNESS.

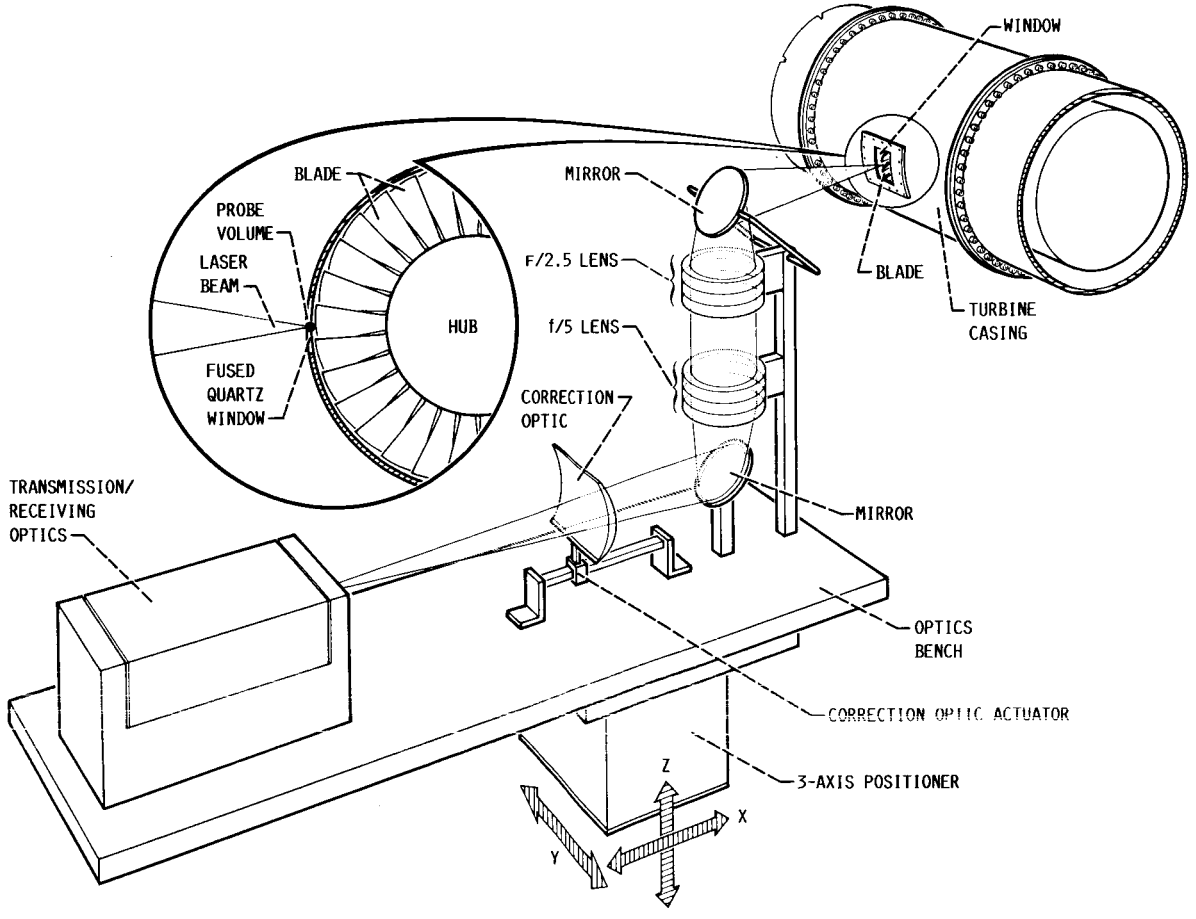

FIGURE 11. - SCHEMATIC VIEW OF A LASER ANEMOMETER SYSTEM APPLIED TO A TURBINE RIG INCORPORATING A CURVE CASING WINDOW. THE ABERRATIONS INDUCED BY THE TURBINE WINDOW ARE COMPENSATED FOR BY THE CORRECTION OPTIC. AS THE 3-AXIS TABLE SCANS THE PROBE VOLUME THROUGH THE BLADE PASSAGE, THE CORRECTION OPTIC POSITION IS ADJUSTED BY ANOTHER ACTUATOR. IN THIS POSITION, THE PROBE VOLUME IS JUST INSIDE THE TURBINE WINDOW, AND THE ACTUATOR IS AT ITS FURTHEST POSITION FROM THE F/5 LENS.

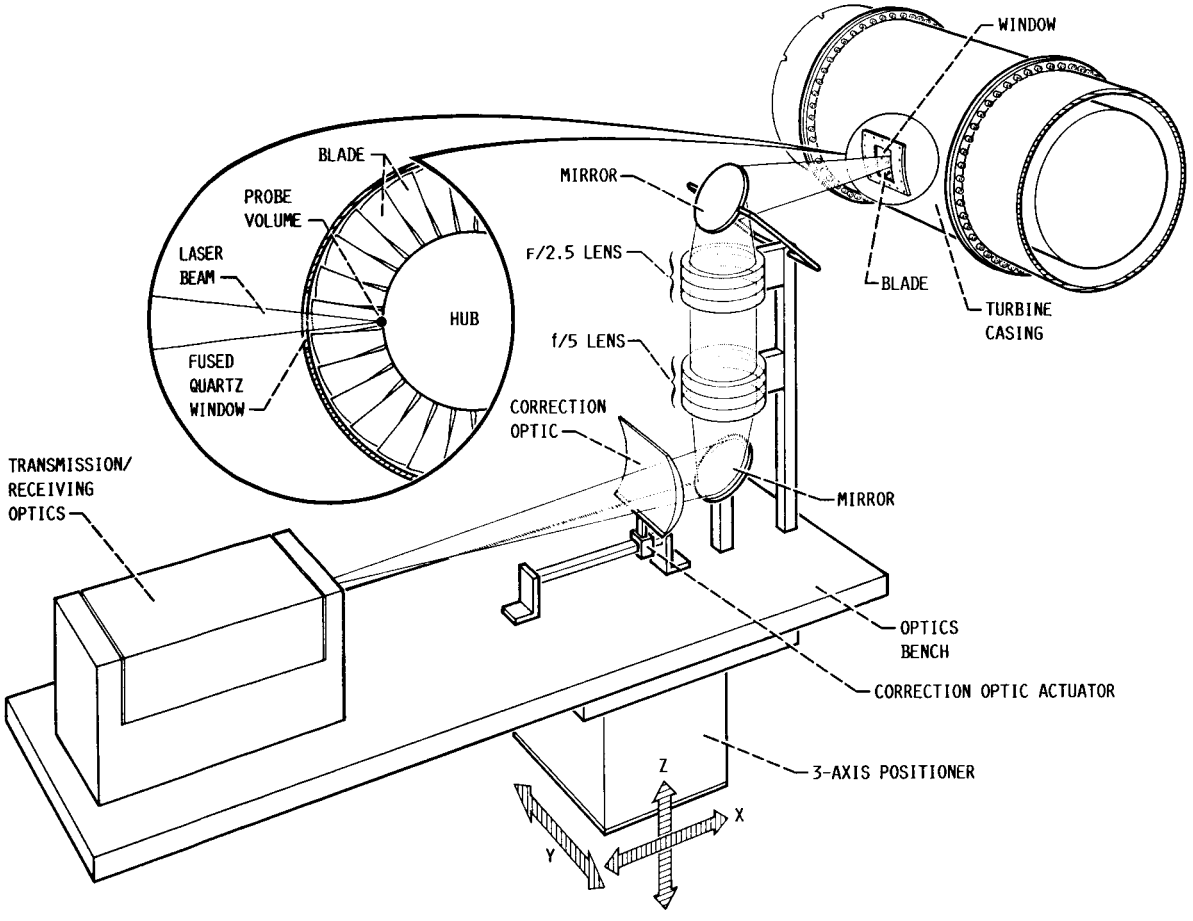

FIGURE 12. - SCHEMATIC OF THE CORRECTED OPTICAL SYSTEM SHOWING A NEW ZOOM POSITION. IN THIS CONFIGURATION, THE PROBE VOLUME IS AT THE ROTOR HUB, AND THE ACTUATOR IS AT ITS CLOSEST POSITION TO THE F/5 LENS.

1. Report No.	2. Government Accession No.	3. Recipient's Catalog No.
NASA TM-88972		

4. Title and Subtitle	5. Report Date
Four Spot Laser Anemometer and Optical Access Techniques for Turbine Applications	6. Performing Organization Code: 533-04-11
7. Author(s): Mark P. Wernet	8. Performing Organization Report No.: E-3440
	10. Work Unit No.
9. Performing Organization Name and Address: National Aeronautics and Space Administration, Lewis Research Center, Cleveland, Ohio 44135	11. Contract or Grant No.
12. Sponsoring Agency Name and Address: National Aeronautics and Space Administration, Washington, D.C. 20546	13. Type of Report and Period Covered: Technical Memorandum
	14. Sponsoring Agency Code

15. Supplementary Notes

Prepared for the 12th International Congress on Instrumentation in Aerospace Simulation Facilities cosponsored by the IEEE Aerospace and Electric Systems Society and NASA Langley Research Center, Williamsburg, Virginia, June 22-25, 1987.

16. Abstract

A new time-of-flight anemometer (TOFA) system, utilizing a spatial lead-lag filter for bipolar pulse generation has been constructed and tested. This system, called a Four Spot Laser Anemometer, was specifically designed for use in high speed, turbulent flows in the presence of walls or surfaces. The new TOFA system uses elliptical spots to increase the flow acceptance angle to be comparable with that of a fringe type anemometer. The tightly focused spots used in the Four Spot yield excellent flare light rejection capabilities. Good results have been obtained to 75 μm normal to a surface, with an f/2.5 collecting lens. This system is being evaluated for use in a warm turbine facility. Results from both a particle lag velocity experiment and boundary layer profiles will be discussed. In addition, an analysis of the use of curved windows in a turbine casing will be presented. Curved windows, matching the inner radius of the turbine casing, preserve the flow conditions, but introduce astigmatic aberrations. A correction optic has been designed that virtually eliminates these astigmatic aberrations throughout the intrablade survey region for normal incidence.

17. Key Words (Suggested by Author(s))	18. Distribution Statement
Laser anemometry Nonintrusive measurements	Unclassified - unlimited STAR Category 35

19. Security Classif. (of this report)	20. Security Classif. (of this page)	21. No. of pages	22. Price*
Unclassified	Unclassified	14	A02

*For sale by the National Technical Information Service, Springfield, Virginia 22161